Journal of Solid State Chemistry 184 (2011) 2701–2706

Contents lists available at SciVerse ScienceDirect

Journal of Solid State Chemistry

journal homepage: www.elsevier.com/locate/jssc

An improved pyrolysis route to synthesize carbon-coated CdS quantum dots with fluorescence enhancement effect

Kejie Zhang, Xiaoheng Liu *

Key Laboratory for Soft Chemistry and Functional Materials of Ministry Education, Nanjing University of Science and Technology, Nanjing 210094, China

ARTICLE INFO

Article history:
Received 8 June 2011
Received in revised form
21 July 2011
Accepted 10 August 2011
Available online 16 August 2011

Keywords:
Carbon-coated CdS quantum dots
Composite
Core-shell structure
Fluorescence enhancement effect

ABSTRACT

Well-dispersed carbon-coated CdS (CdS@C) quantum dots were successfully prepared via the improved pyrolysis of bis(1-dodecanethiol)-cadmium(II) under nitrogen atmosphere. This simple method effectively solved the sintered problem resulted from conventional pyrolysis process. The experimental results indicated that most of the as-prepared nanoparticles displayed well-defined core-shell structures. The CdS cores with diameter of ~5 nm exhibited hexagonal crystal phase, the carbon shells with thickness of ~2 nm acted as a good dispersion medium to prevent CdS particles from aggregation, and together with CdS effectively formed a monodisperse CdS@Carbon nanocomposite. This composite presented a remarkable fluorescence enhancement effect, which indicated that the prepared nanoparticles might be a promising photoresponsive material or biosensor. This improved pyrolysis method might also offer a facile way to prepare other carbon-coated semiconductor nanostructures.

1. Introduction

Due to the quantum size effect, semiconductor quantum dots (QDs), especially the II–VI semiconductor QDs, exhibit size-dependent optical properties [1], which are of great importance in various applications such as biological labels, optoelectronic devices, and solar cells [2–5]. As an important direct-band semiconductor with a bandgap of 2.4 eV, CdS QDs have been widely applied in optoelectronic devices [6]. The size-dependent optical properties of CdS QDs imply that CdS QDs with different fluorescence characteristics can be prepared just by tailoring their size. Therefore, it is a remarkable topic for materials scientists using simple and efficient routes to prepare the size-controlled CdS QDs. Generally, CdS QDs is most often synthesized through the combination of cadmium and sulfur precursors in the presence of a QDs-binding ligand that stabilizes the growing quantum dots and prevents their aggregation into bulk CdS in liquid solution [7–10]. However, the colloidal CdS QDs in aqueous solution usually had a wide size distribution [11], and a defect-related photoluminescence (PL) band was dominant [12].

Pyroloysis method, including flame aerosol synthesis and flame spray synthesis, was industrially the most successful and low-cost synthesis method to prepare all kinds of nanomaterials [13]. As a convenient and inexpensive method, pyrolysis technique can also be used to synthesize inorganic nanomaterials with multifarious morphologies from complexes [14–19]. For example, transition–metal complexes (usually organometallic compounds and clusters) acting as single-source precursors can be used to prepare chalcogenide nanomaterials [16,18]. However, the conventional pyrolysis method usually leads to sintered products with uncontrollable particle sizes, which will have a great effect on the unique properties of quantum dots. Some improved pyrolysis methods such as metallorganic chemical vapor deposition [3], aerosol-assisted chemical vapor deposition [20], reducing flame spray synthesis [21] and atmospheric pressure chemical vapor deposition [22] have been applied to fabricate semiconductor nanoparticles, but it still remains a key research challenge to develop the convenient, economical and efficient pyrolysis methods.

On the basis of our knowledge, few works have been reported on the preparation of carbon-coated CdS (CdS@C) QDs by a conventional pyrolysis of a single precursor in the solid phase. Several benefits motivated us to prepare CdS@C nanocomposite by an improved organometallic pyrolysis reaction route. Firstly, an appropriate organometallic complex (bis(1-Dodecanethiol)-cadmium (II) $Cd(C_{12}H_{25}S)_2$) was selected as a single precursor, which included Cd, S and C elements. The complex not only promoted the formation of CdS QDs, but also avoided other impurities into CdS@C QDs. Secondly, monodisperse CdS@C QDs could be directly obtained by an improved pyrolysis method, which included conventional pyrolysis process and acid treatment process. Thirdly, the acid-treatment technique effectively solved the sintered problem of the conventional pyrolysis method [23]. Fourthly, compared with wet chemical or chemical vapor deposition method, the improved pyrolysis method was a simple and economical technique.

In this work, we successfully fabricated well-defined monodisperse CdS@C QDs from $Cd(C_{12}H_{25}S)_2$ ($Cd(DM)_2$) by the improved pyrolysis method. As expected, sintered CdS was

* Corresponding author. Fax: +86 25 84315054.
E-mail address: xhliu@mail.njust.edu.cn (X. Liu).

0022-4596/$ - see front matter © 2011 Elsevier Inc. All rights reserved.
doi:10.1016/j.jssc.2011.08.011

removed by acid-treatment process, which effectively solved the sintered problem of the conventional pyrolysis. Interestingly, the as-synthesized nanocomposite showed obvious quantum confinement and fluorescence enhancement effects compared with the bulk CdS. This method might also offer a facile way to prepare other carbon-coated semiconductor nanostructures.

2. Experimental section

2.1. Preparation of CdS@C QDs

$Cd(C_{12}H_{25}S)_2$ ($Cd(DM)_2$) was prepared by the method described in a previous paper [24]. $Cd(DM)_2$ was heated directly in a horizontal muffle furnace from room temperature to 500 °C and was kept at this temperature for 2 h in N_2. Then the sintered product was obtained, which consisted of orange and black particles. After immerging the sintered product in hydrochloride acid aqueous solution (HCl, volume fraction: 12%) for 30 min, with the orange particles disappearing, the black colloid precipitates (namely the acid-treated sample) were collected by filtering and washing with distilled water.

For comparison, the pure CdS nanoparticles with a diameter of ~5 nm were prepared by conventional chemical deposition method.

2.2. Characterization of the products

The phase and purity of as-obtained products were examined by an X-ray diffraction (XRD, Bruker D8 advance) operating at 40 kV and 40 mA, using Cu $K\alpha$ radiation (λ=1.54 Å). The morphology characterization and structure analysis were carried out by scanning electron microscopy (JSM-5610LV, FESEM) and transmission electron microscopy (JEOL-2100, TEM), respectively. The composition of the sintered product was analyzed by an energy dispersive X-ray spectrometer (EDX) attached to FESEM. Raman spectra (RS) were run on a Renishaw Raman microscope with 514.5 nm provided by an Ar^+ laser. The composition analysis of the acid-treated sample and the electronic binding energy were examined on an X-ray photoelectron spectroscope (XPS, Thermo ESCALAB 250), with Al $K\alpha$ (1486.7 eV) radiation for excitation (15 kV and 10 mA). The X-ray source was operated at 150 W. The C 1*s* peak at a binding energy 284.7 eV was taken as an internal standard. Solid-state fluorescence measurements (λ_{ex}=250 nm) were recorded from 270 to 480 nm on a FL3-TCSPC fluorescence spectrophotometer using 3 nm slit width.

3. Results and discussion

X-ray diffraction measurement was performed to probe the structure and phase purity of the samples. As shown in Fig. 1a, the XRD peaks of the sintered product could be well indexed to hexagonal CdS (JCPDS No. 06-0314). Because the strong peaks of CdS covered the diffraction peaks of carbon, typical XRD peaks of carbon could not be observed in Fig. 1a. For the acid-treated sample, XRD pattern consisted of weak CdS peaks and wide amorphous carbon XRD responsed at 20–30° are shown in Fig. 1b. The intensities of the peaks of the acid-treated sample were weaker than that of the sintered sample, which implied that some uncoated CdS crystals with high crystallinity were removed by the acid-treatment process.

Raman scattering spectroscopy was employed to further discuss the nanostructures of carbon-coated CdS QDs. Fig. 2 depicts the room-temperature Raman spectra of the sintered product and

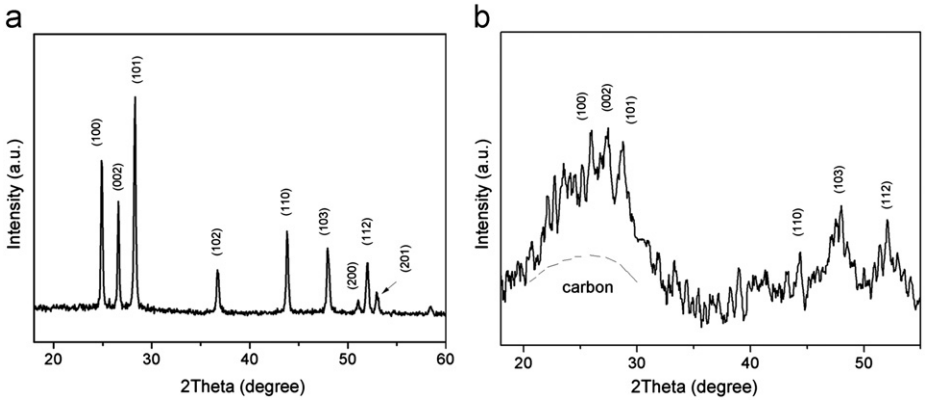

Fig. 1. XRD patterns of the samples: (a) the sintered product and (b) the acid-treated sample.

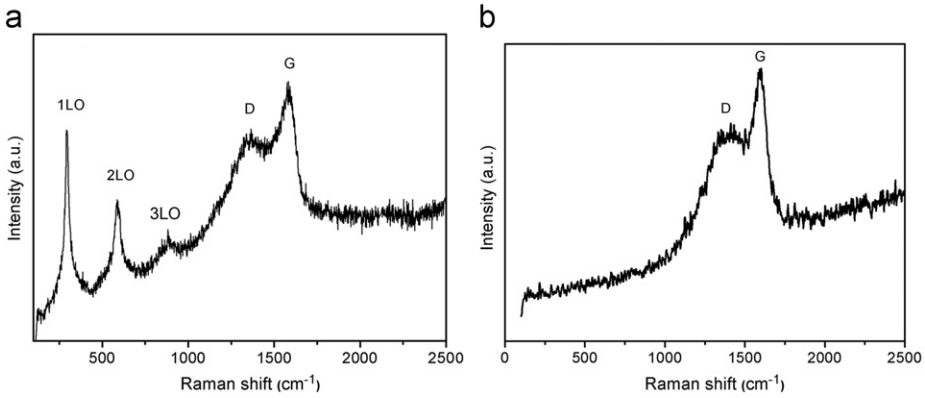

Fig. 2. Raman spectra of the samples: (a) the sintered product and (b) the acid-treated sample.

the acid-treated sample. The Raman spectrum of the sintered product (in Fig. 2a) displayed three peaks at ~292, ~587 and ~881 cm^{-1}, which, respectively, corresponded to the first-, second- and third-order LO phonon modes of CdS nanoparticles [25–27]. Compared with pure CdS [28], the Raman peaks of the sintered product exhibited obvious red shift, with the 1LO~14 cm^{-1}, 2LO~27 cm^{-1} and 3LO~26 cm^{-1}, respectively. The red shift phenomena were possibly attributed to the confinement of optical phonons in the nanometer-size samples, as demonstrated by a spatial correlation model [29]. In an infinite crystal, only phonons near the center of the Brillouin zone ($q \approx 0$) could contribute to the Raman mode because of momentum conservation between phonons and incident light. On the other hand, in a finite crystal such as a QD, the phonons could be confined in space by crystal boundaries or defects (for QDs the confinement was mainly due to the nanoscale dimensions in the radial direction). This resulted in uncertainty in the phonon momentum, and allowed phonons with $q \neq 0$ to contribute to Raman scattering, leading to a variation in the peak position and width of the Raman signals [30]. In addition, a possible reason might be attributed to the interaction between coated CdS QDs and carbon shell [31]. All of the above factors influenced the Raman activity of CdS nanoparticles. From the spectrum of the acid-treated sample in Fig. 2b, it could be seen that there were two Raman peaks at ~1363 and ~1581 cm^{-1}, corresponding to the D and G peaks of carbon [32], respectively. Compared with the sintered product, the acid-treated sample only showed the D and G peaks of carbon and no peaks of CdS, which implied that uncoated CdS particles were removed by HCl, and the CdS nanoparticles in the acid-treated sample were completely coated by carbon. This was in good agreement with the above XRD analysis results. The XRD and Raman results indicated that acid-treatment effectively removed the sintered CdS particles.

The FESEM image of the sintered product (Fig. 3a) shows that the most CdS@C QDs are spherical nanoparticles. Coated and uncoated CdS nanoparticles sintered together. In Fig. 3b, quantitative energy-dispersive X-ray analysis (EDS) obtained from several crystals revealed the surface elemental composition (Cd, S and C) and a S/Cd ratio of 1:1, within the error of EDS.

Fig. 4a–c displays the TEM images of the acid-treated sample with different magnification, while Fig. 4b is the magnification of partial Fig. 4a. All of three figures show that there are lots of highly monodisperse and homogeneous CdS QDs in the acid-treated sample. Carbon shell served as a good dispersion medium to form monodisperse CdS QDs. This coating action of carbon shell prevented aggregation of CdS QDs and reduced their surface defects, which was consistent with the following XPS and PL results. Fig. 4(d) is the high resolution TEM image of an individual CdS QD coated by carbon, which shows a well-defined core-shell structure. The coated CdS QD was a crystalloid core with a diameter of ~5 nm and the corrugated carbon was a thin shell with a thickness of ~2 nm. TEM results provided additional evidence that the sintered CdS particles were effectively removed by the acid-treatment procedure and the well-defined monodisperse CdS@C QDs were obtained.

The XPS survey spectra of the acid-treated sample are shown in Fig. 5. The identified peaks were labeled to various corresponding elements. Fig. 5a shows the full XPS spectrum taken from the surface of CdS@C QDs nanoparticles. The peaks in the XPS data could be identified to originate from Cd, S, C and O elements. The O peaks stemmed from the atmospheric contamination. The binding energies obtained in the XPS analysis were corrected in consideration of the specimen charging and by referring to O1*s* at 530.7 eV. In the high-resolution XPS spectrum of CdS@C nanoparticles, the binding energy of Cd 3*d* doublet was located at 405.4 eV and 411.8 eV, with the peak separation of 6.4 eV (Fig. 5b). Similarly, the peak position of S 2*p* was located at 161.5 eV and 162.6 eV (Fig. 5c), but the separation was very small (~1.1 eV). It was obvious that there was a slight shift in the Cd 3*d* peaks (from 405.5 to 405.4 eV, 412.2 to 411.8 eV) and S 2*p* peaks (from 165 to 161.5 eV) to lower binding energy comparing with their standard values reported in the literature for CdS [33–35]. The possible reason was that Cd atoms were afforded the electrons from carbon shell, which caused the electron density around Cd atoms to increase and the strength of the Cd–S bond to decrease [34]. Therefore, the binding energies of Cd 3*d* and S 2*p* were reduced. This implied that there was an interaction between C shell and CdS nanoparticles, which might result in the forming of CdS@C QDs composite. Therefore, XPS results provided additional evidence of the existence of CdS@C nanomaterial, which agreed with the results of XRD, RS and TEM. Fig. 5d shows that the peak position of C 1*s* is located at 284.7 eV. As the shell, the carbon passivated the surface of coated CdS QDs and reduced their surface defects [36], which might improve the fluorescent property of CdS@C QDs. This could be confirmed by the following PL results.

The possible formation mechanism of CdS@C QDs is proposed based on the above analysis. A schematic illustration of their formation process is as follows.

In order to solve the problem of the severe agglomeration of CdS particles during the pyrolysis process, we treated the sintered product using HCl, illustrated in Fig. 6. The method was composed of two steps: (i) pyrolysis and (ii) acid treatment processes. The pyrolysis step (at 500 °C) involved three sub-processes. In the first step, all the C–S bands were broked, the CdS nanoparticles and the ligand fragments were formed. As a result, some CdS nanoparticles were fully coated with the fragments, and others were uncoated. And then, further pyrolysis process resulted in the carbonization of the ligand fragments to form carbon shell, which is coated on the CdS particles. At the same time, uncoated CdS

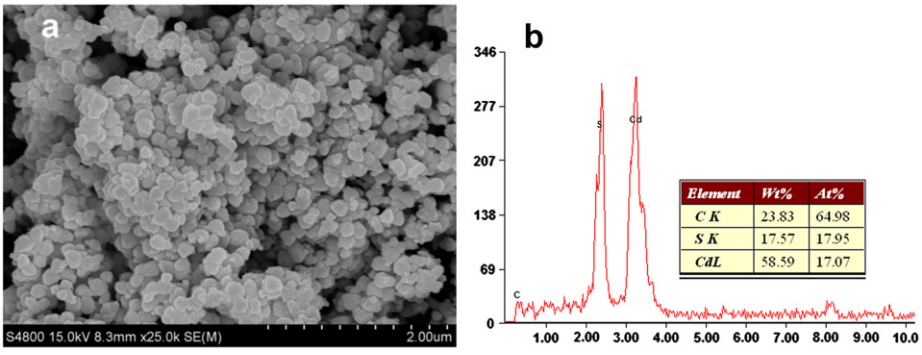

Fig. 3. (a) FESEM image and (b) EDS image of the sintered product.

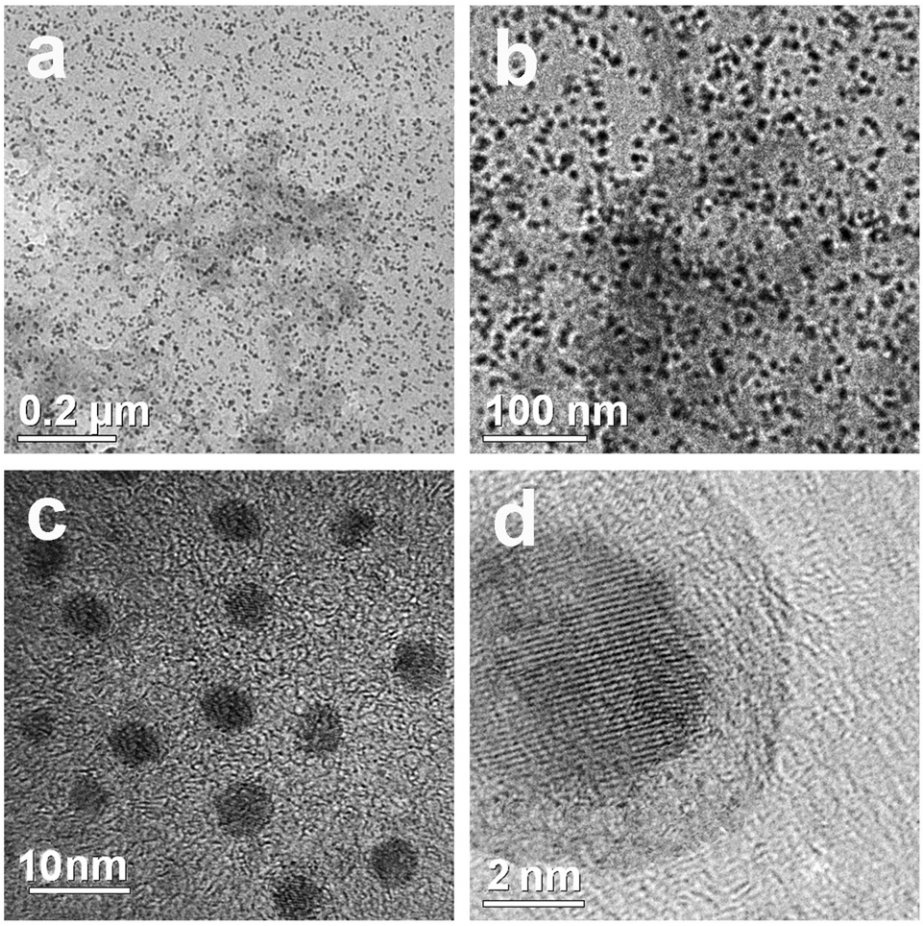

Fig. 4. TEM images of different magnifications of the acid-treated sample: HRTEM image of a core-shell CdS@C QDs nanoparticle.

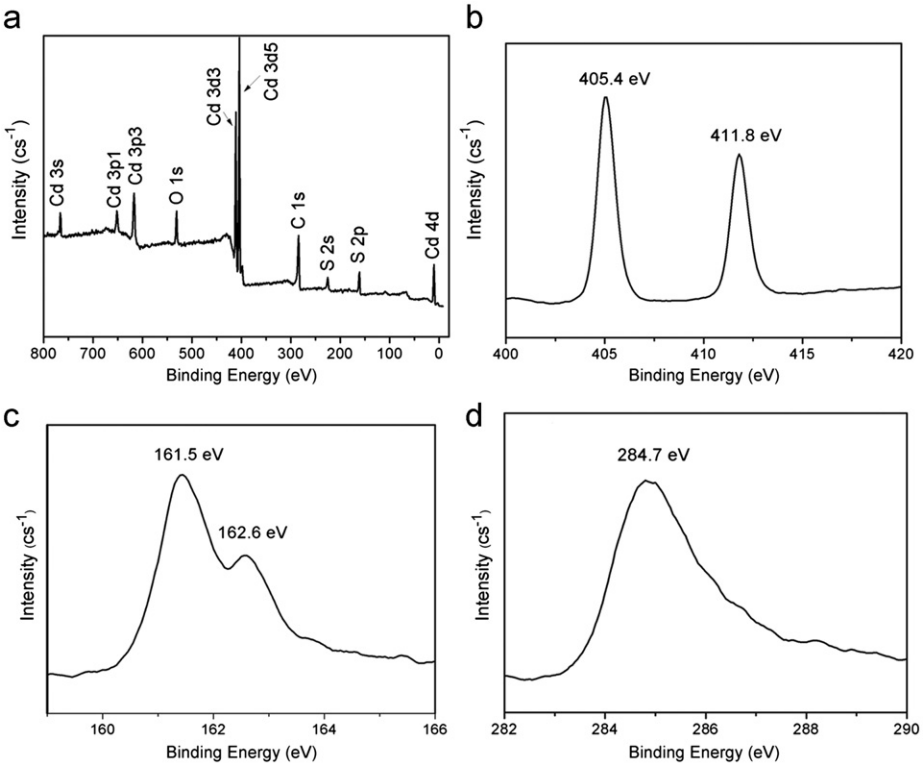

Fig. 5. Full XPS spectrum obtained from the surface of the acid-treated sample (a), narrow-scan XPS spectra of Cd 3*d* (b), S 2*p* (c) and C 1*s* (d) from the sample (a).

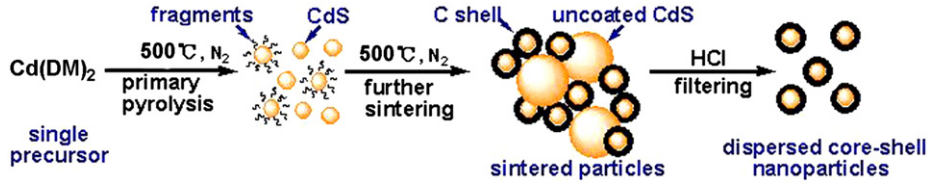

Fig. 6. Schematic illustration of the formation process of CdS@C QDs obtained from improved pyrolysis of $Cd(DM)_2$.

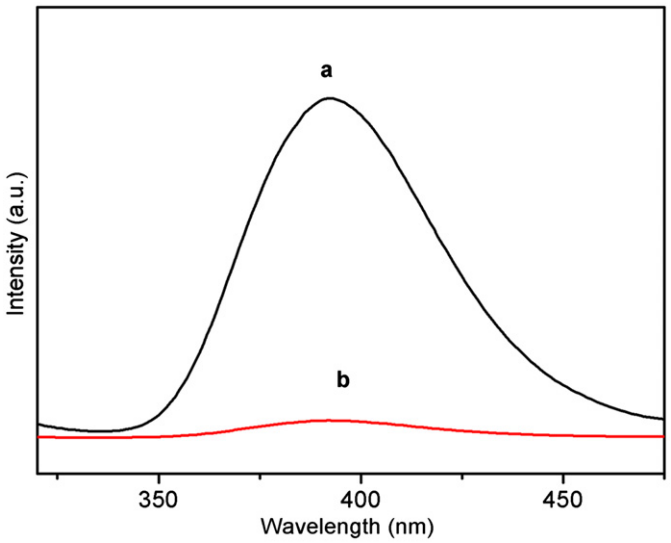

Fig. 7. PL spectra of (a) the acid-treated sample and (b) the pure CdS nanoparticles with an excitation wavelength of 250 nm.

particles grew up to larger crystals. Finally the coated and uncoated CdS particles sintered and formed to the larger hardened aggregates. In the second step, the uncoated CdS particles were removed by the acid treatment process and the monodisperse carbon-coated CdS QDs were obtained. It was easily inferred that the carbon shell prevented the coated CdS QDs from being etched by HCl and enhanced their mono-dispersion.

Room temperature solid-state photoluminescence (PL) fluorescence (exited with 250 nm laser) measurement results are shown in Fig. 7. The PL spectra of the acid-treated sample and the as-prepared pure CdS nanoparticles showed a strong emission band at ~392 nm. The characteristic emission band was ascribed to CdS excimer band-to-band emission [37], which was obviously blue-shifted from that of the bulk CdS (512 nm) [38]. The significant blue shift was attributed to the strong quantum confinement effects of CdS QDs. Comparing with the acid-treated sample, the peak intensity of the pure CdS QDs was obviously decreased. In other words, the fluorescence intensity of the acid-treated sample was ~5 times that of the pure CdS nanoparticles. However, previous research suggested that CdS loaded on graphene presented fluorescence quenching compared with the pure CdS [39]. The possible reasons were as follows. Firstly, carbon displayed a plasmon resonance absorption and changed the radiative decay rate of CdS QDs [40], which could make CdS QDs fluorescence enhancement. Secondly, compared with the pure CdS, carbon passivated the surface of CdS particles, reduced their surface defects and non-radiative transitions, which might result in the fluorescence enhancement of CdS QDs [36,41]. Thirdly, with the nanoshell system [42], carbon shells were largely non-conducting, which helped to enhance the quantum yield of CdS QDs [43]. In addition, CdS QDs were well monodisperse in carbon, bringing in the reduction of the CdS particles' higher density of surface states, which might lead to the fluorescence enhancement of CdS QDs. With the good property, CdS@C QDs maybe act as selective ion probes for ion analysis in volume-limited biological samples and single cells [44].

4. Conclusions

We developed a facile approach to synthesize well-dispersed carbon-coated CdS quantum dots using $Cd(DM)_2$ as the single precursor via the improved pyrolysis technique. The sintered problem resulted from the conventional pyrolysis method was effectively solved by acid treatment process through removing uncoated CdS particles. The individual well-defined CdS@C QDs had core diameters of ~5 nm and shell thicknesses of ~2 nm. The CdS@C QDs composite exhibited obviously strong quantum confinement and fluorescence enhancement effects, which implied that the CdS@C QDs might be a promising candidate for novel optoelectronic devices. Consequently, carbon shell was a good dispersion medium to form monodisperse CdS QDs and carbon coating was an effective method to improve optoelectronic performance of CdS QDs. The proposed approach gives a new avenue for producing carbon-based semiconductor quantum dots materials.

Acknowledgments

This project is supported financially by the Natural Science Foundation of China (grant No. 20974045) and the Natural Science Foundation of Jiangsu Province (No. BK2009385).

References

[1] A.P. Alivisatos, Science 271 (1996) 933–937.
[2] K. Sato, Y. Tachibana, S. Hattori, T. Chiba, S. Kuwabata, J. Colloid Interf. Sci. 324 (2008) 257–260.
[3] D. Fan, M. Afzaal, M.A. Mallik, C.Q. Nguyen, P. O'Brien, P.J. Thomas, Coord. Chem. Rev. 251 (2007) 1878–1888.
[4] M. Shalom, S. Rühle, I. Hod, S. Yahav, A. Zaban, J. Am. Chem. Soc. 131 (2009) 876–9877.
[5] A. Datta, S.K. Panda, S. Chaudhuri, J. Phys. Chem. C 111 (2007) 17260–17264.
[6] T.A. Pham, B.C. Choi, Y.T. Jeong, Nanotechnology 21 (2010) 465603–465609.
[7] J. Mao, J.-N. Yao, L.-N. Wang, W.-S. Liu, J. Colloid Interf. Sci. 319 (2008) 353–356.
[8] X. Liu, Y. Jiang, X. Lan, S. Li, D. Wu, T. Han, H. Zhong, Z. Zhang, J. Colloid Interf. Sci. 354 (2011) 15–22.
[9] M. Naito, K. Iwahori, A. Miura, M. Yamane, I. Yamashita, Angew. Chem. Int. Ed. 49 (2010) 7006–7009.
[10] X. Li, Y. Gao, L. Yu, L. Zheng, J. Solid State Chem. 183 (2010) 1423–1432.
[11] S. Brichkin, E. Chernykh, High Energy Chem. 45 (2011) 1–12.
[12] D. Kim, M. Miyamoto, T. Mishima, M. Nakayama, J. Appl. Phy. 98 (2005) 083514.
[13] E.K. Athanassiou, R.N. Grass, W.J. Stark, Aerosol Sci. Technol. 44 (2010) 161–172.
[14] L. Friebe, K. Liu, B. Obermeier, S. Petrov, P. Dube, I. Manners, Chem. Mater. 19 (2007) 2630–2640.
[15] M.A. Malik, M. Afzaal, P. O'Brien, Chem. Rev. 110 (2010) 4417–4446.
[16] K. Ramasamy, M.A. Malik, J. Raftery, F. Tuna, P. O'Brien, Chem. Mater. 22 (2010) 4919–4930.
[17] D. Chen, F. Zhao, H. Qi, M. Rutherford, X. Peng, Chem. Mater. 22 (2010) 1437–1444.
[18] T. Mirkovic, M.A. Hines, P.S. Nair, G.D. Scholes, Chem. Mater. 17 (2005) 3451–3456.

[19] E.K. Athanassiou, R.N. Grass, W.J. Stark, Nanotechnology 21 (2010) 215603–215609.
[20] S.S. Garje, D.J. Eisler, J.S. Ritch, M. Afzaal, P. O'Brien, T. Chivers, J. Am. Chem. Soc. 128 (2006) 3120–3121.
[21] E.K. Athanassiou, R.N. Grass, W.J. Stark, Nanotechnology 17 (2006) 1668–1673.
[22] I. Cesar, A. Kay, J.A. Gonzalez Martinez, M. Grätzel, J. Am. Chem. Soc. 128 (2006) 4582–4583.
[23] I.K. Herrmann, R.N. Grass, D. Mazunin, W.J. Stark, Chem. Mater. 21 (2009) 3275–3281.
[24] S. Banerji, R.E. Byrne, S.E. Livingstone, Trans. Met. Chem. 7 (1982) 5–10.
[25] X.-P. Shen, A.-H. Yuan, F. Wang, J.-M. Hong, Z. Xu, Solid State Commun. 133 (2005) 19–22.
[26] T. Zhai, X. Fang, Y. Bando, Q. Liao, X. Xu, H. Zeng, Y. Ma, J. Yao, D. Golberg, ACS Nano 3 (2009) 949–959.
[27] A. Pan, R. Liu, Q. Yang, Y. Zhu, G. Yang, B. Zou, K. Chen, J. Phys.Chem. B 109 (2005) 24268–24272.
[28] C.A. Arguello, D.L. Rousseau, S.P.S. Porto, Phys. Rev. 181 (1969) 1351–1363.
[29] Z.Q. Wang, J.F. Gong, J.H. Duan, H.B. Huang, S.G. Yang, X.N. Zhao, R. Zhang, Y.W. Du, Appl. Phys. Lett. 89 (2006) 033102–033103.
[30] B. Cao, Y. Jiang, C. Wang, W. Wang, L. Wang, M. Niu, W. Zhang, Y. Li, S.-T. Lee, Adv. Funct. Mater. 17 (2007) 1501–1506.
[31] F. Li, Y. Bao, J. Chai, Q. Zhang, D. Han, L. Niu, Langmuir 26 (2010) 12314–12320.
[32] A.C. Ferrari, J.C. Meyer, V. Scardaci, C. Casiraghi, M. Lazzeri, F. Mauri, S. Piscanec, D. Jiang, K.S. Novoselov, S. Roth, A.K. Geim, Phys. Rev. Lett. 97 (2006) 187401–187404.
[33] X.L. Tong, D.S. Jiang, Z.M. Liu, M.Z. Luo, Y. Li, P.X. Lu, G. Yang, H. Long, Thin Solid Films 516 (2008) 2003–2008.
[34] R.S. Vemuri, S.K. Gullapalli, D. Zubia, J.C. McClure, C.V. Ramana, Chem. Phys. Lett. 495 (2010) 232–235.
[35] M.T.S. Nair, P.K. Nair, J. Appl. Phys. 75 (1994) 1557–1564.
[36] C.L. Wang, H. Zhang, J.H. Zhang, M.J. Li, K. Han, B. Yang, J. Colloid. Interf. Sci. 294 (2006) 104–108.
[37] L. Spanhel, M. Haase, H. Weller, A. Henglein, J. Am. Chem. Soc. 109 (1987) 5649–5655.
[38] C.B. Murray, D.J. Norris, M.G. Bawendi, J. Am. Chem. Soc. 115 (1993) 8706–8715.
[39] P. Wang, T. Jiang, C. Zhu, Y. Zhai, D. Wang, S. Dong, Nano Res. 3 (2010) 794–799.
[40] J.R. Lakowicz, Anal. Biochem. 337 (2005) 171–194.
[41] W. Chen, Z.G. Wang, Z.J. Lin, L.Y. Lin, Solid State Commun. 101 (1997) 371–375.
[42] T. Yamaguchi, T. Kaya, H. Takei, Anal. Biochem. 364 (2007) 171–179.
[43] E.K. Athanassiou, F. Krumeich, R.N. Grass, W.J. Stark, Phys. Rev. Lett. 101 (2008) 166804–166808.
[44] Y. Chen, Z. Rosenzweig, Analy. Chem. 74 (2002) 5132–5138.